One-step “green” synthesis of dispersable carbon quantum dots/poly (methyl methacrylate) nanocomposites for tribological applications

Maria Sarno[a,b,*], Waleed Ahmed Abdalglil Mustafa[c], Adolfo Senatore[b,c], Davide Scarpa[c]

[a] *Department of Physics “E.R. Caianiello”, University of Salerno, Via Giovanni Paolo II, 132, 84084, Fisciano (SA), Italy.*
[b] *NANO_MATES, Research Centre for Nanomaterials and Nanotechnology at the University of Salerno, University of Salerno, Via Giovanni Paolo II, 132, 84084, Fisciano (SA), Italy.*
[c] *Department of Industrial Engineering, University of Salerno, Via Giovanni Paolo II, 132, 84084, Fisciano (SA), Italy.*

Abstract

Herein, the production of a poly (methyl methacrylate)/carbon quantum dots (PMMA/CQDs)-based composite has been proposed for the first time through a one-step, mild temperature, easily scalable oleic acid- and citric acid-based green synthesis. The composite consists of an oil-compatible polymer matrix which locally releases anti-friction and anti-wear CQDs under lubrication conditions. After extensive characterization, tribological tests were performed in commercial VG 220 at different temperatures, loads and additive concentrations, showing remarkable performance. At 25°C and under a 19 N normal pressure, with 0.3 wt.% PMMA/CQDs, 20.2 % and 41.6 % reductions were observed for friction and wear, respectively. Furthermore, viscosities measurements at both 40°C and 100°C showed that the nanocomposite presence did not substantially interfere with the oil rheological parameters.

Keywords: new synthesis approach; oil compatible PMMA/CQDs; friction and wear reduction.

*Corresponding authors: Tel.: +39 089 963460; fax: +39 089 964057; E-mail address: msarno@unisa.it (M. Sarno).

1. Introduction

In the last few decades, the demand for highly efficient and environmentally sustainable lubricant oils is becoming more and more imperative. Conventional lubrication of operating machines is carried out by use of different types of liquid lubricants, which act as intermediate means between the sliding metallic surfaces. Along with the base oil, additives are typically added in order to increase tribological performance. Some of the most adopted ones are friction modifiers (FM) and anti-wear (AW) additives, which have been represented for many years by P-, Mo- and S-containing compounds [1-3]. However, since these additives have by now reached their performance limits, and in the view of enhancing the system efficiency, reducing harmful compounds emission and environmental impact as well, nanoparticles have been considered as the most feasible and effective alternative [4-7]. Their higher lubricating performance is strictly connected to their intrinsic characteristics such as small size (≤100 nm), morphology and thermal stability which permit them to function within lubrication surface interfaces with a greater durability even under harsher conditions [8] compared to conventional FM and AW additives. Furthermore, nanoparticles morphology and structure can be accurately manipulated for superior results. Among nano-additives, carbon-based nanomaterials are capable of ensuring high anti-wear and anti-friction performance [9] as a result of their chemical inertness, as well as of their remarkable mechanical and structural properties, and through several effective friction mechanisms such as rolling, protective film, self-mending and polishing effects [10-16]. However, the inert structure of nano-carbons and their solid nature, especially for 1D and 2D materials, makes their long-time dispersions in lubricant oil extremely challenging [17] With the aim of increasing carbon nano-additives stability, surface-modification processes have been proposed, even though they still hinder large-scale applications because of their high cost, complexity and, even more, poor effectiveness [18-21].

Carbon quantum dots (CQDs) can be regarded as a new type of nano-carbons consisting of quasi-spherical particles with ultra-small sizes and unique optical and electronic properties. Since their accidental discovery by Xu et al. in 2004 [22], CQDs have been receiving a significant research focus. Other than sizes below 10 nm, they often exhibit a polar nature due to the presence of functionalized hydroxyl and carboxyl groups on their surface, and are highly biocompatible and environmental friendly [23,24].

An additional advantage of CQDs is the ease of synthesis as they can be prepared from natural carbonaceous sources under both severe and mild conditions, for instance through carbonization of various fruit juices, vegetables, fruit peels, plant parts and citric acid [25-30].

As lubricant additives, in virtue of their ultra-small size and "naturally" functionalized structure, CQDs exhibit enhanced tribological properties, even though they stably disperse only in polar solvents [31,32]. Indeed, the polar nature of CQDs poses the question of their compatibility with non-polar hydrocarbon oils, such as polyalphaolefin (PAO) and mineral oils, which highly hampers the future usage of CQDs with them. In this direction, a few attempts have been made so far [33,34], yet there is still the need to search for simpler synthesis procedures which do not involve the usage of harmful substances.

On the other hand, in order to obtain complete and effective lubricant formulations, researchers often seek for additives which can be multifunctional as well as compatible with different chemicals in a formulation, both with other additives as well as the base fluid. Within this context, the development of multifunctional additives with wear- and friction-reducing properties as well as viscosity index-improving behavior, which do not interfere either with each other or with the base oil, yet exhibit beneficial synergistic interactions, would be of high significance.

Poly (methyl methacrylate) (PMMA) is considered as one of the most efficient viscosity index (VI) improvers for base lubricant oils, i.e. able to significantly reduce the lubricant oil viscosity dependence on temperature variations. Non-polar oil-compatible PMMA is traditionally synthesized through free radical polymerization of alkyl methacrylate monomers. [35]. According to the most widely reported mechanism of how this polymer acts as viscosity modifier, PMMA increases the base oil viscosity proportionately with temperature due to the expansion of its long molecular chains with increasing temperatures [36]. Indeed, chains occupying a larger volume possess higher resistance to flow, hence greater viscosity [37].

As far as literature is concerned, few papers have been published on the preparation of CQDs/PMMA nanocomposites [38-40], in which two step synthesis mechanisms were employed to obtain CQDs, subsequently incorporated in a polymer matrix to give nanocomposites films. In particular, Aziz et al. [38] reported the preparation, for applications in optoelectronic devices, of PMMA/CQDs nanocomposite films in two steps: (1) synthesis of CQDs by hydrothermal treatment using glucose, H_3PO_4 and NaOH as well as chloroform in the purification step; (2) preparation of the nanocomposite using a solution casting procedure carried out by mixing PMMA/acetone and CQDs/acetone solutions. Similarly, Maxim et al. [39] reported an improvement of the light harvesting performance in perovskite solar cells by adopting CQDs-embedded PMMA thin films obtained in a two-steps procedure: (1) phosphorus-doped CQDs were prepared at 200°C for 1 h starting from Na_2HPO_4 and dextrose; (2) afterwards, CQDs with sizes around 3–7 nm were mixed with PMMA in chlorobenzene. Eventually, Bouknaitir et al. [40] studied the optical and the dielectric properties of nanocomposite based on the incorporation of CQDs in PMMA at several

filler loading. The CQDs were synthesized at a temperature up to 300°C, in the presence of octadecene acting as non-coordinating solvent. The nanocomposite was prepared by drop-casting a PMMA/chloroform solution and the prepared CQDs onto glass slides.

Herein, with the aim to improve the sustainability and the simplicity of CQDs synthesis process, which thus far involved harmful molecules, as well as in order to enhance CQDs dispersion stability in non-polar lubricant oils by simultaneously obtaining an effective multifunctional nano-additive for tribological applications, the production of PMMA/CQDs composites, consisting of CQDs covered by an extremely thin layer of PMMA, was proposed for the first time by means of a one-step, mild temperature, oleic acid- and citric acid-based *green* synthesis. In particular, no harmful oleic acid was chosen as solvent of the one-step *green* process, contributing to drastically reduce detrimental environmental impact in favour of an improved simplicity and, therefore, feasibility in view of process industrialization. The synthesis of CQDs occurred during the thermal expansion of PMMA molecular chains, followed by nanoparticles entrapment within the polymer body after cooling. The resulting product is an oil-compatible polymer matrix which will locally release anti-friction and anti-wear CQDs under lubrication conditions.

After an extensive characterization, tribological tests were carried out in a commercial mineral oil, confirming the enhanced performance of the sample.

2. Materials and methods

2.1 PMMA/CQDs composite, CQDs and t-PMMA preparation and dispersion in oil

Citric acid (CA, purity grade ≥99.5%), crystalline poly (methyl methacrylate) (PMMA) and oleic acid (OA, purity grade 90%) were all purchased from Sigma Aldrich. As for the PMMA/CQDs composite, 5g of CA were dissolved in 50 ml of bi-distilled water and mixed with 100 ml of OA, which is used a solvent to guarantee the proper reaction environment. Afterwards, 0.5g of PMMA in powder form was added to the mixture, which was then heated up to 200˚C for 2 h and under magnetic stirring in an open flask. The flask was maintained opened to allow water evaporation. The synthesis of CQDs occurred during the thermal expansion of PMMA molecular chains, followed by nanoparticles entrapment within the polymer body after cooling (as shown in Figure 1).

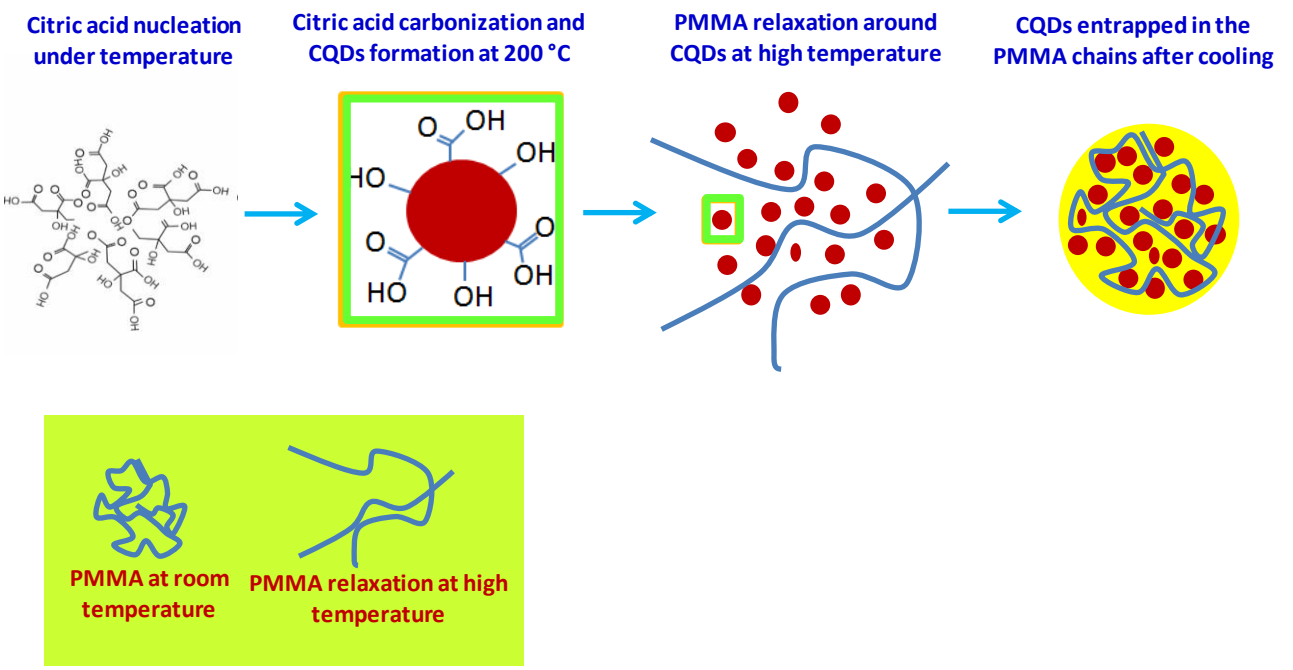

Figure 1. Illustrative representation of formation and entrapment of CQDs within PMMA structure.

Furthermore, for comparison reasons, two other samples were synthesized: a treated PMMA sample and a PMMA-free carbon quantum dots sample, named as t-PMMA and CQDs in the following study, respectively. As for t-PMMA, it was prepared with the same procedure without the addition of CA. On the other hand, CQDs were obtained with both OA and CA without the addition of PMMA. After reaction occurred, the three mixtures were cooled down to room temperature and then underwent centrifugation at 7500 rpm and 5˚C. The resulting solid particles were rinsed with ethanol for several times and eventually dried for 24 h at 60˚C. After synthesis, PMMA/CQDs and t-PMMA were both dispersed at 0.1 wt.% into a VG 220 base oil (Mineral oil, viscosity index = 93, density at 15 °C = 891.1 kg/m^3) by means of a 400 W tip sonicator at for 2h at maximum power. CQDs do not disperse well in the oils because of their polar nature. In Figure 2, the pictures of the base oil VG 220 and the PMMA/CQDs composite dispersed in VG 220 are shown.

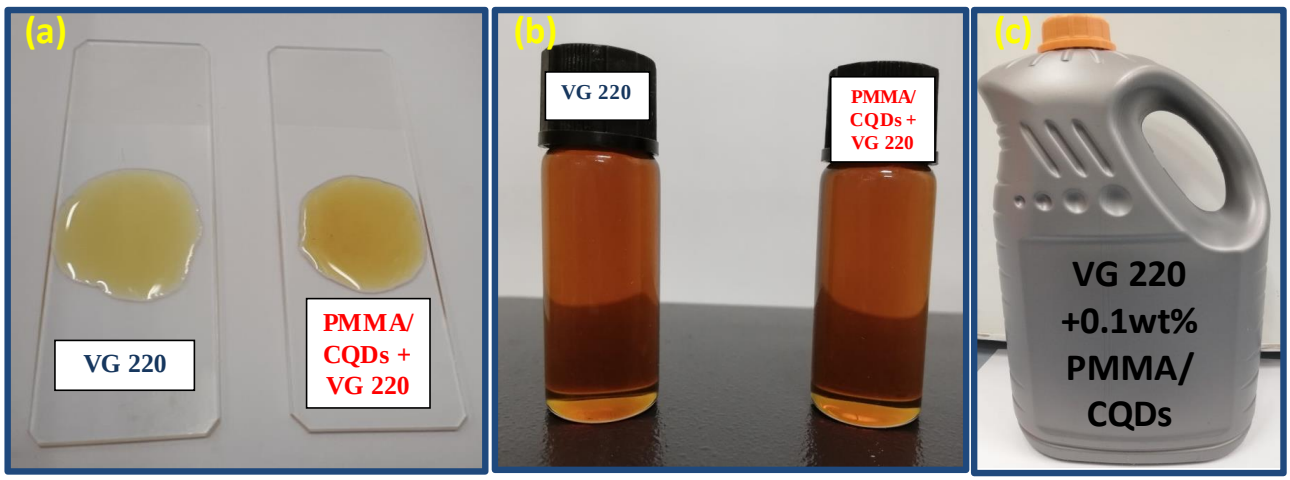

Figure 2. Photos: of pure VG 220 oil and PMMA/CQDs dispersed in VG 220 oil (a) and (b); of one tank containing added oil for high volume tribological characterization.

2.2 PMMA/CQDs composite, CQDs and t-PMMA characterization

Transmission electron microscopy (TEM) by means of a FEI Tecnai 200 kV electron microscope was used for understanding the morphological characteristics of both the samples. The absorbance of the supernatant produced after centrifugation was then evaluated through Thermo-Scientific UV–vis Evolution Q60 spectrophotometer. FT-IR analysis was carried out through a Vertex 70 apparatus (Bruker Corporation) by adopting the KBr technique. Thermogravimetric analysis (TGA) and Derivative Thermogravimetry analysis (DTG) were performed through a SDTQ 600 Analyzer (TA Instruments) under the following conditions: heating rate of 10 °C/min, from room temperature up to 450 °C under air flow. Particle size distribution of nanosheet dispersion was determined using a dynamic light scattering (DLS) instrument (HPPS ET - Malvern Instruments). Eventually, Raman spectra were obtained by means of a Renishaw inVia spectrometer at a wavelength of 514 nm.

2.3 Tribological test description

In order to perform tribological tests, a Ducom TR-BIO-282 tribometer was adopted. In detail, the equipment consists of a tribopair composed by an upper steel ball (X45Cr13 polished steel ball, 52-54 HRC, diameter of 6 mm) in reciprocating motion and a lower X210Cr12 steel disc (60 HRC, roughness R_a of 0.30 μm, diameter of 25 mm, thickness of 6 mm) completely flooded in a lubricant bath. Reciprocating sliding tests were performed with a normal load equal to 19 N and an initial average Hertzian contact pressure of 1.17 GPa at 25 °C and 80 °C. Afterwards, normal pressure was increased to 58 N and average Hertzian contact pressure to 1.76 GPa and measurements performed at 25 °C [41,42].

Such test conditions were chosen to explore the anti-friction and anti-wear behaviour of CQDs as mineral oil additive in both boundary and mixed lubrication regimes. With sliding motion set at 5mm stroke and 10 Hz as frequency, boundary regime at zero-speed inversion points moves to mixed conditions in each stroke by sweeping the Stribeck number in the range [0, $7.38\ 10^{-12}$ m] at room temperature, and [0, $1.85\ 10^{-12}$ m] at 80 °C; the transition to fully thin-film lubrication regime is expected at around $1.0\ 10^{11}$ m, outside of the domain of the test herein discussed.

3. Results and discussion

3.1 Characterization results

TEM analysis was adopted for a better understanding of CQDs morphology with and without the presence of PMMA. Figure 3a, 3b and 3c show TEM images of the CQDs at different

magnifications, revealing semi-spherical particles with an average diameter of 3 nm, as clarified by the particle size distribution in Figure 3d.

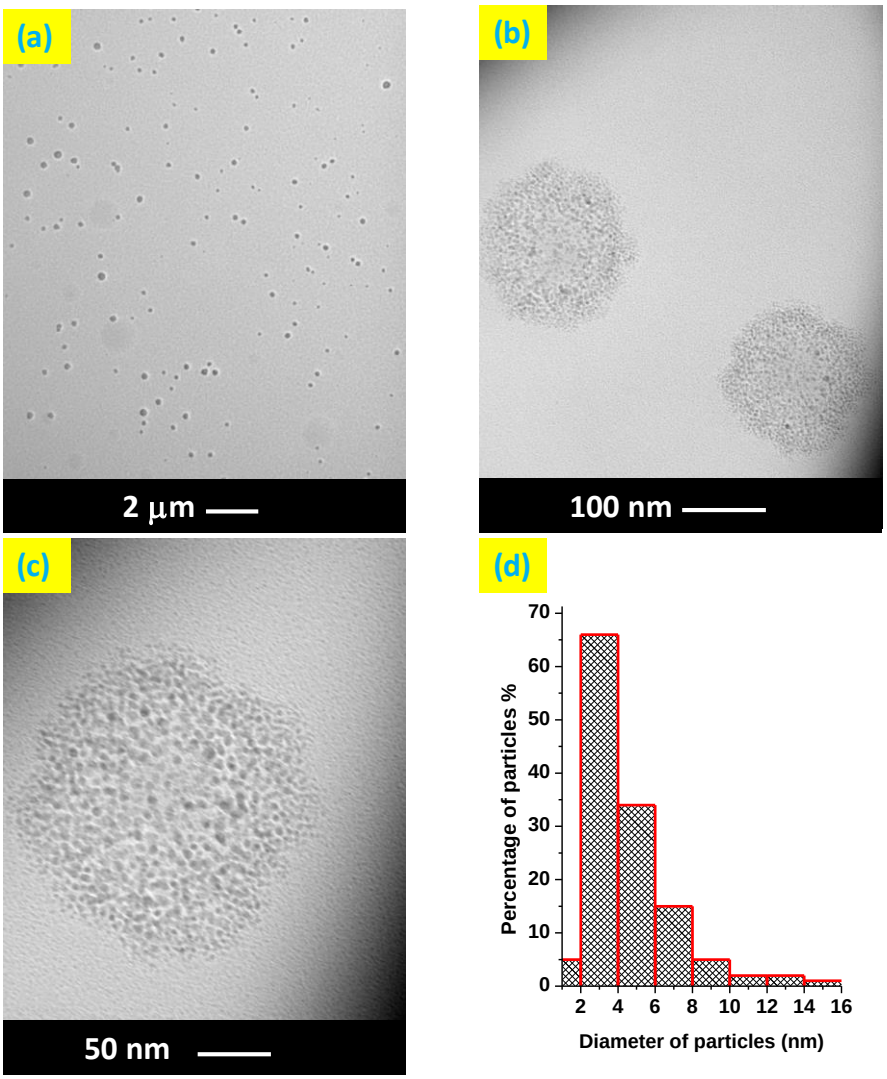

Figure 3. TEM images of the formed CQDs at different magnifications: 2µm scale bar (a); 100 nm scale bar (b); and, 50 nm scale bar (c). The particle size distribution of the formed dots (d).

Furthermore, in the presence of PMMA, the synthesized CQDs have smaller average diameters (Figure 4). Moreover, it is possible to observe the higher distance between each individual particle (Figure 4b).

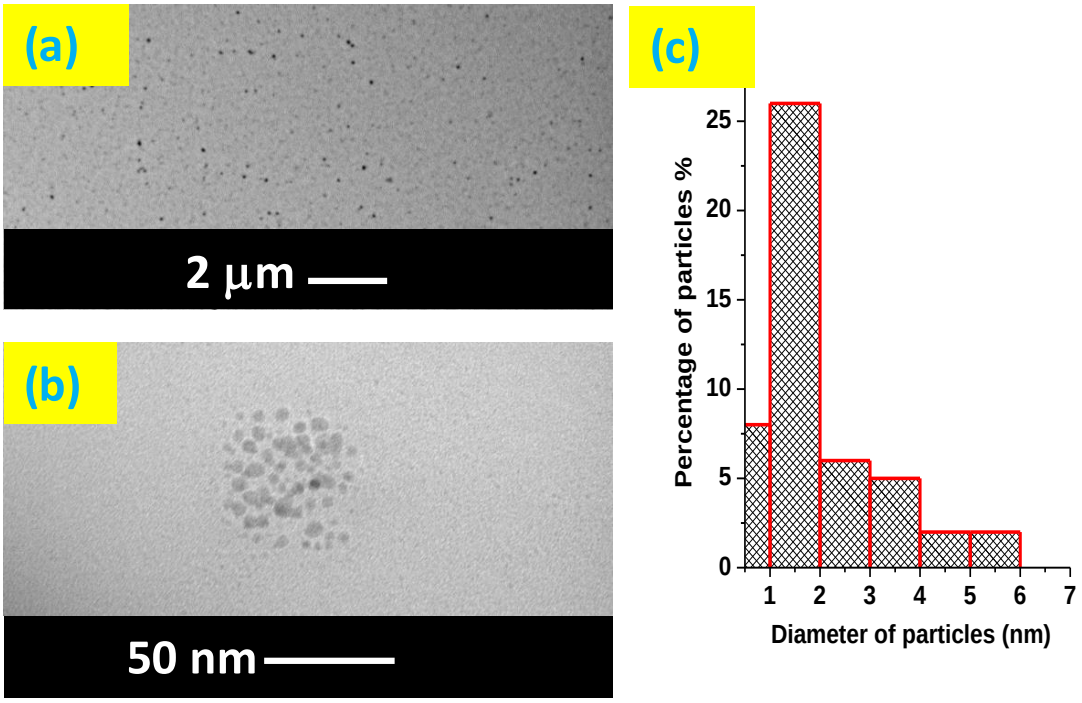

Figure 4. TEM images of the PMMA/CQDs at different magnifications: 2µm scale bar (a); 50 nm scale bar (b). The particle size distribution of the formed CQDs (c).

Hydrodynamic diameters in solution were determined by DLS. The DLS technique measures Brownian motion (the random movement of particles due to the bombardment by the solvent molecules which surround them) and relates this to the size of the particles. The size of a particle is calculated from the translational diffusion coefficient by using the Stokes-Einstein equation [43]. The hydrodynamic diameters are in the range 1-18 nm for CQDs centered at 3 nm and in the range 3-10 nm centered at 4 nm for the PMMA-covered CQDs (Figure 5). These results are consistent with the microscopy observations, indicating a mean shell of PMMA of about 2 nm covering the dots.

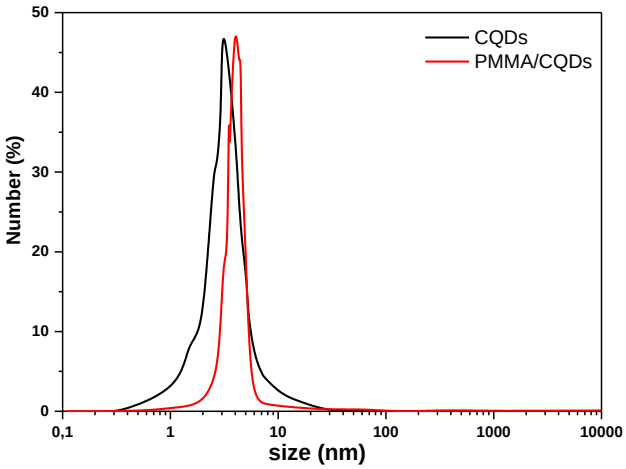

Figure 5. PSD of CQDs and PMMA/CQDs as determined by DLS technique.

The typical UV-Vis spectrum of the CQDs is reported in Figure 6a, showing that the main absorption band can be seen at 340 nm, which suggests the formation of quantum dots with a size in the range 2-4 nm [44] in agreement with TEM analysis. In Figure 6b and 6c, the spectra of t-PMMA and of PMMA/CQDs are reported. The absorption band displayed by the pure treated PMMA is around 274 nm, that corresponds to the n-π* electronic transition bands [45] exerted by the non-bonding electrons [46]. On the other hand, the shift of PMMA absorbance in the presence of CQDs to a higher wavelength (297 nm) indicates the formation of CQDS in the PMMA matrix that can be likely attributed to either the interaction between the quantum dots and the polymer chains or the formation of extra defects in the energy band gap [47,48]. In addition, Figure **6**d shows the behavior of pure ethanol (on the left) and CQDs dispersed in ethanol (on the right) while being exposed to a UV lamp: contrarily to the one on the left, the sample on the right exhibits fluorescence properties, thus confirming the successful formation of carbon quantum dots.

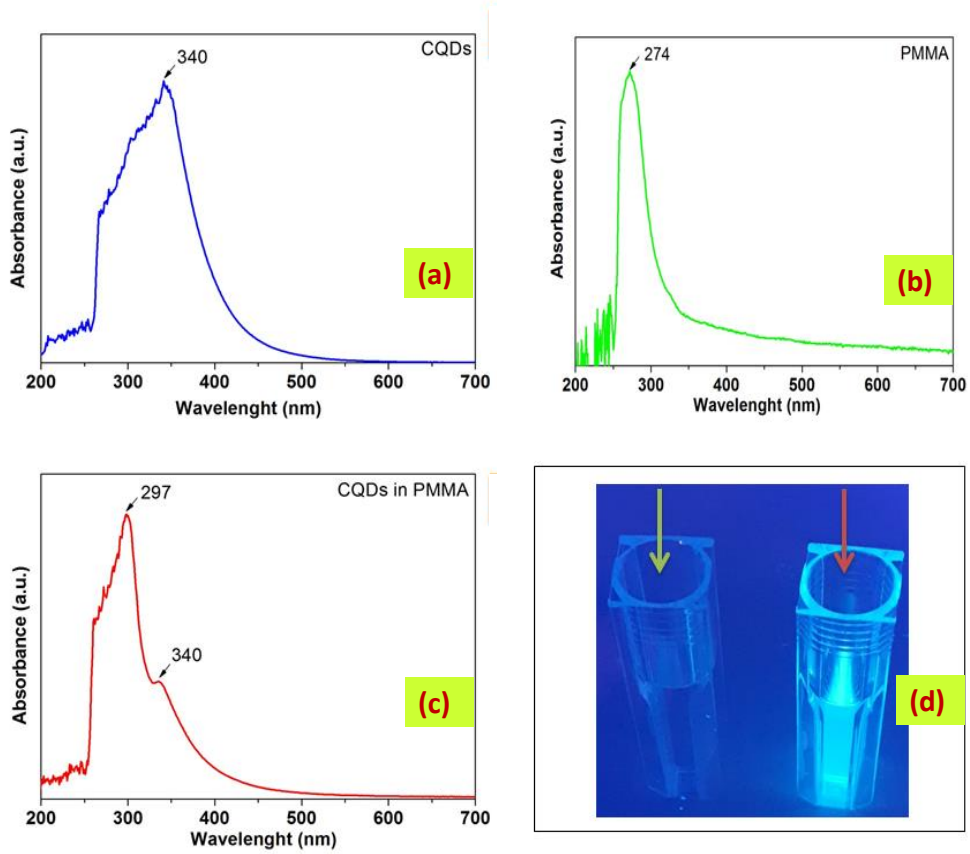

Figure 6. UV-vis spectra of the different samples (a) for CQDs, (b) for the t-PMMA and (c) for PMMA/CQDs; (d) the picture represents ethanol (yellow arrow, on the left) and CQDs dispersed in ethanol (red arrow, on the right), evidencing the fluorescence properties of the latter.

The FT-IR spectral investigation was conducted and the results shown in Figure **7**. Both spectra of CA and PMMA/CQDs composite display stretching vibrations over 1700 cm^{-1} which are due to carboxylic free groups of CA (green spectrum) and –COOH on the surface of CQDs (blue spectrum). On the other hand, PMMA shows a band at 1730 cm^{-1} due to ester carbonyl stretching, which is no more visible in the spectrum of PMMA/CQDs, suggesting a shift as previously reported for PMMA and carbon quantum dots nanocomposite films formed by solution casting method [**49**]. This phenomenon can indicate a polymer conformational change at molecular level [**50**]. PMMA/CQDs composite revealed C=C bond vibrations at 1460 cm^{-1}. The bands at 2928 cm^{-1} and 2858 cm^{-1} are due to $–CH_3$ and $–C_2H_2–$ groups, respectively. Moreover, stretching vibrations at 3498 cm^{-1} strongly present in CA, are entirely disappeared in the PMMA/CQDs composite, indicating the complete dehydration and decomposition of CA during reaction.

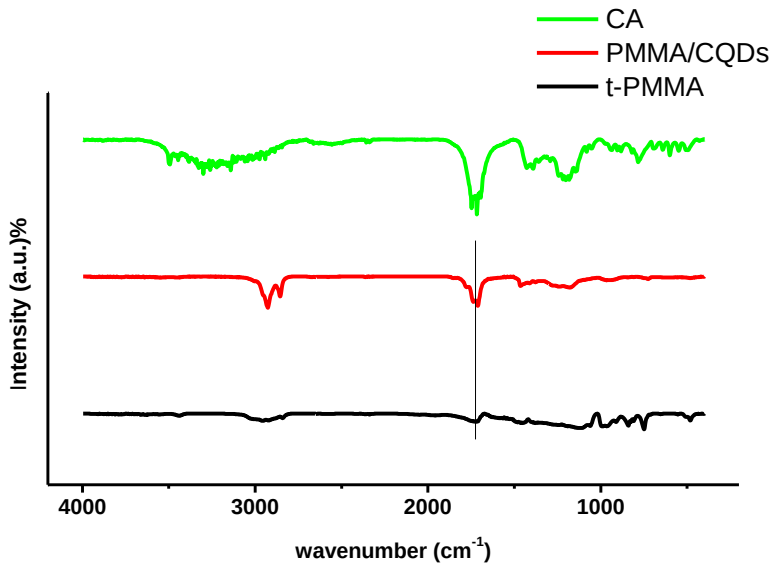

Figure 7. FT-IR spectra of citric acid, PMMA/CQDs and t-PMMA.

The analyses of the thermograms of PMMA/CQDs and of t-PMMA are reported in Figure 8. The thermogravimetric profile of PMMA/CQDs exhibits a first weight loss of ~55 wt. % (onset at 167.9 °C), probably due to CQDs [51]. On the other hand, the presence of CQDs stabilizes PMMA, whose weight loss occurs in the temperature range 322 °C-431 °C, at higher temperatures than PMMA alone.

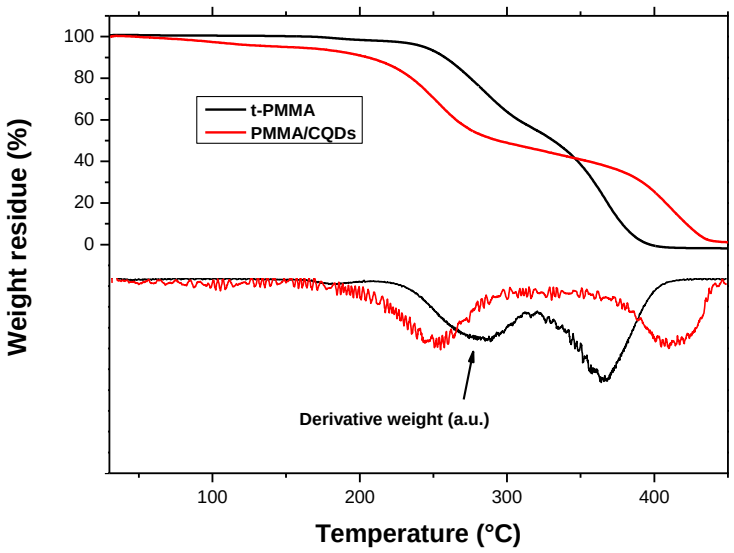

Figure 8. TGA and DTG graphs of PMMA/CQDs and t-PMMA.

3.2 Tribological performance

The friction and wear performance of VG 220 base oil, along with VG 220 with 0.1 wt.% of PMMA/CQDs and VG 220 with 0.1 wt.% of t-PMMA, are shown in Figure **9**. The additive concentrations were selected on the basis of the optimum concentration of nano-additives in various studies on nano-lubricants [52-55] and with a view to promoting stability and modifying as little as possible the base oil, which must still be added in a delicate balance with other components, e.g. antioxidant and antifoam improvers, etc. What is more, tribological tests were not performed on CQDs sample because of its weak dispersion in oil. In particular, the coefficient of friction (CoF) and wear scar diameter (WSD) values of the pure base oil with PMMA/CQDs and t-PMMA, measured under ambient temperature and low-load tests conditions, are reported in Figure 9a. As also summarized in Figure 10, which includes further evaluations at 0.3 wt.% and 0.5 wt.% of PMMA/CQDs in oil, at the optimum concentration of 0.3 wt.%, minimum CoF and WSD values were recorded of 20.2 % and 41.6 % reductions, respectively. It is worth noticing that these remarkable values were recorded under mixed lubrication conditions in which, because of the relatively high thickness of oil between lubricated mechanical parts, the anti-wear and anti-friction properties of the additive cannot be fully exploited and enhanced as in the boundary lubrication regime often explored in literature.

A similar trend was observed when the test temperature was raised up to 80 ˚C (Figure **9**b): a minor improvement in tribological performance, but more significant at this high temperature in which the reduction of the oil viscosity highlights the role of the nanoadditive, with a reduction of 10% and 12 % in CoF and WSD, respectively, for 0.1 wt. % PMMA/CQDs in oil was observed. In order to better understand the role of the nano-additive on the load carrying capacity, the Hertzian pressure

was increased to 1.76 GPa for the same reciprocating test (Figure 9c). In detail, the load carrying capacity was higher for the 0.1 wt. % PMMA/CQDs in comparison with the other two samples, with a reduction of 8% in both CoF and WSD. The variation of CoF versus time was reported in Figure 9d at room temperature for a duration of 120 minutes. The CoF of pure base oil was fluctuating in a uniform manner with average constant values every 20 minutes time intervals. As the CoF starts to decline, it suddenly bounces back again to maintain relatively the same values of the previous period. McFarlane, J. S., & Tabor, D. explained this behavior in terms of "asperity junction growth" [56] that occur when the normal load is high enough on the asperities causing a partial absence of the lubricating media. Additionally, the asperities under load suffer from thermal softening and are pulled off under motion of contacting pairs forming wear debris conjunctions, hence increasing CoF. This behavior can also be observed in the case of t-PMMA sample, but as for the PMMA/CQDs sample there is a gradual reduction in CoF as a function of time as well. Initially, the values of CoF are higher than the ones at the end of the test: this can be attributed to the lack of interactions in the *tribo-zone* with PMMA/CQDs at the beginning. Mungse at al. described a similar phenomenon and the suggested reason is the enhanced dispersion of nanoparticles over time which ensures a continuous supply to the *tribo-interface* and the formation of a uniform *tribo-film* once a certain shear condition is reached [57].

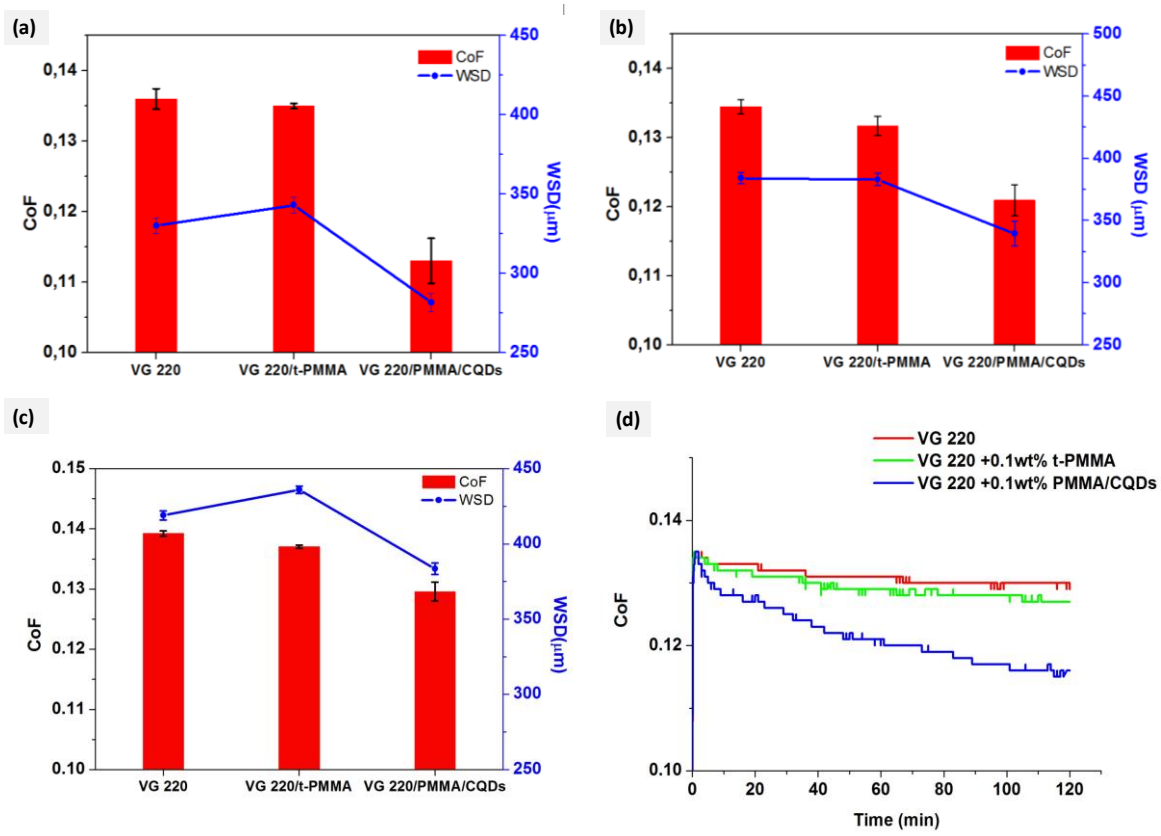

Figure 9. The reciprocating tribometer results of the 1-hour mean CoF and WSD values for pure base oil VG 220, 0.1 wt. % PMMA-t and 0.1 wt. % PMMA/CQDs at: (a) 25°C and at 19 N, 1.17 GPa, (b) 80°C and at 19 N, 1.17 GPa; and (c) 25°C and at 58 N, 1.76 GPa. (d) CoF versus time results for the three different samples at 25°C, at 19 N, 1.17 GPa.

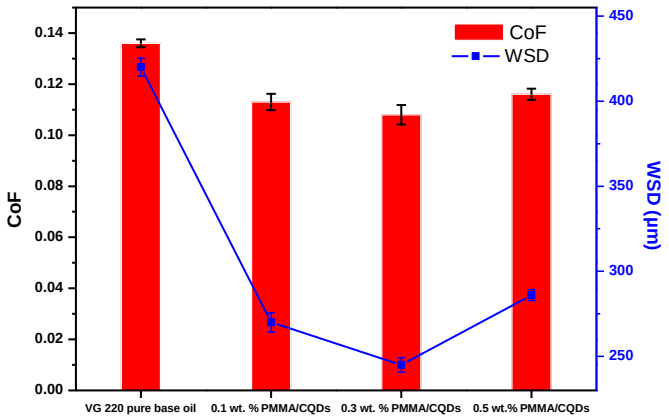

Figure 10. One-hour average CoF and WSD for 0.1 wt. % PMMA/CQDs in VG 220, 0.5 wt. % PMMA/CQDs in VG 220 and pure VG 220 at 25 °C and 19 N.

The wear scars after 60 minutes of test for the 0.1 wt. % PMMA/CQDs + VG 220 oil and the pure VG 220 oil, at ambient temperature, 80 ˚C and at a high normal pressure of 21 N at 25°C are shown in Figure **11**. Moreover, the surface roughness obtained by a Profilometer for the corresponding wear scars is also reported. From the Figure, it can be stated that the presence of the nanocomposite did not only reduce the WSD under all the three conditions, but also significantly smoothened the surfaces after the test.

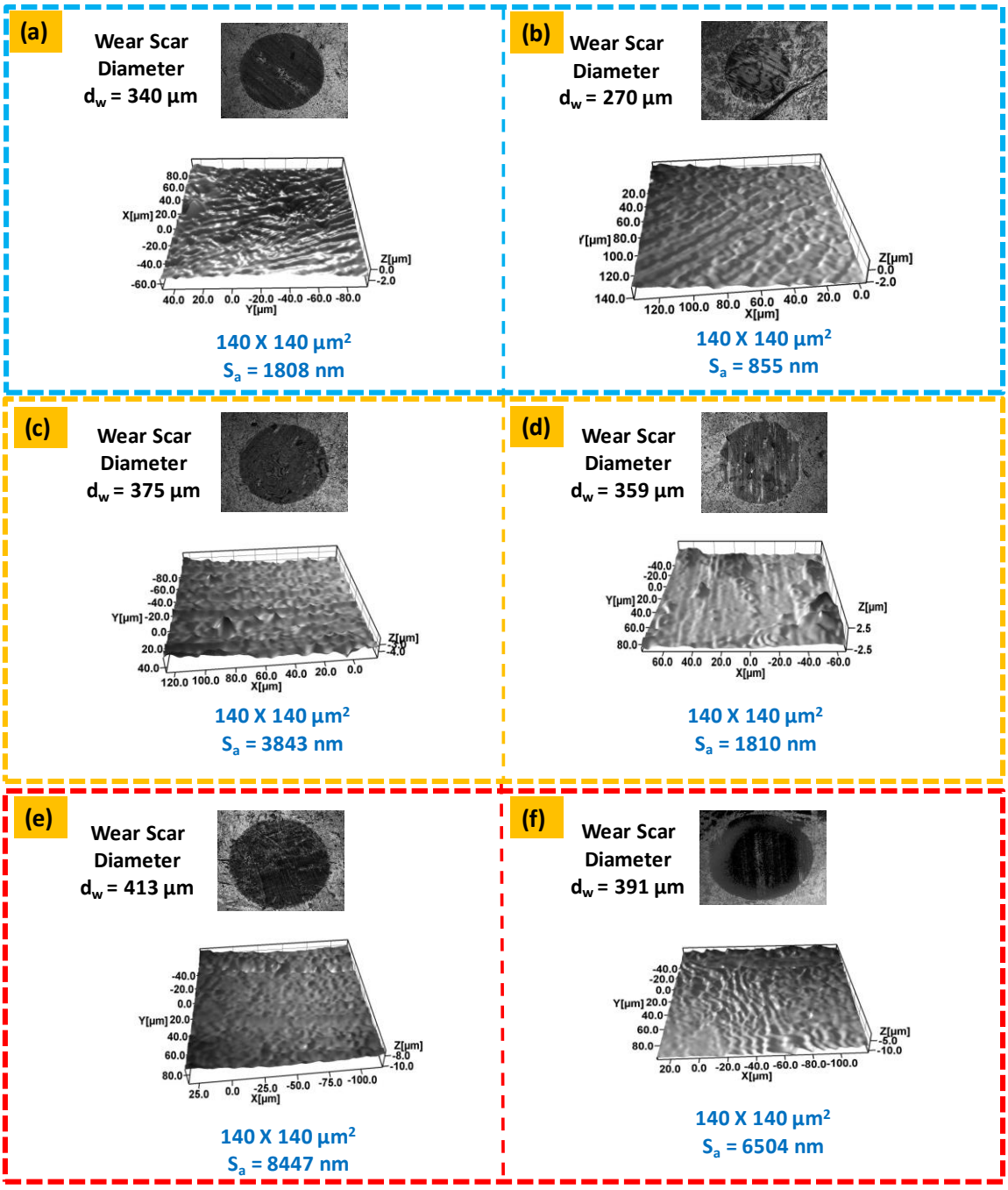

Figure 11. Worn surfaces of steel balls with: (a) VG 220 and (b) 0.1 wt. % PMMA/CQDs at 25°C and at 19 N, 1.17 GPa; VG 220 (c) and 0.1 wt. % PMMA/CQDs (d) at 80°C and at 19 N, 1.17 GPa; (e) VG 220 and (f) 0.1 wt. % PMMA/CQDs at 25 °C and at 58 N, 1.76 GPa.

In Figure 12a, the image of a worn surface lubricated with 0.1 wt. % PMMA/CQDs at 25°C and at 19 N, 1.17 GPa is shown. Micro-Raman spectrometer was further used to analyze the worn surface, trying to identify carbon forms which can be formed by the CQDs. Raman spectra collected in some areas of the image in Figure 12a are reported in Figures 12b, 12c and 12d. In particular, a band at about 700 cm^{-1} can be seen in the light areas, which can be attributable to iron oxides, indicating oxidation on the steel surface, Figure 12b. It was found that in darker areas, the characteristic peaks

of carbon, D and G bands at about 1350 and 1590 cm^{-1}, are clearly visible, Figure 12c. On the other hand, they are less intense in lighted areas, Figure 12d. No well-defined peaks from PMMA were detected on the worn surface. These observations can draw the consideration that carbon derived by CQDs, variously distributed deposits on the contact surfaces, helping lubrication and avoiding oxidation.

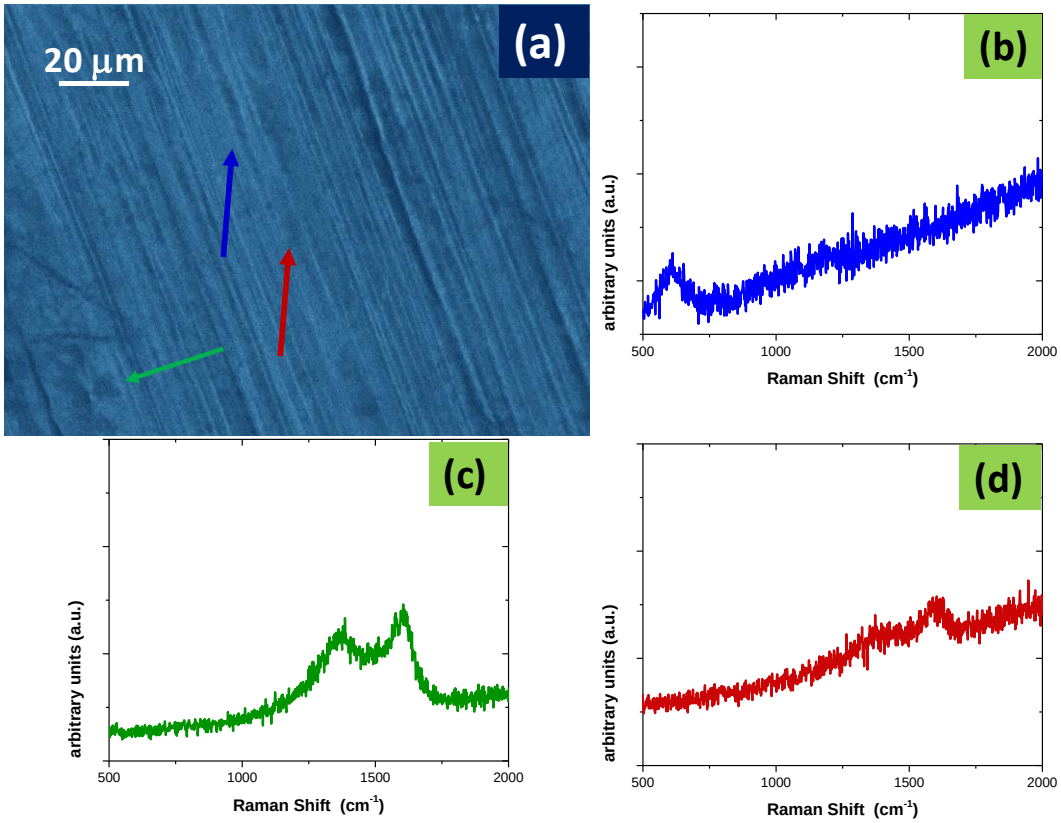

Figure 12. Image of the worm surface lubricated by 0.1 wt. % PMMA/CQDs at 25°C and at 19 N, 1.17 GPa (a). Raman spectra collected in the areas indicated by the arrows (b,c,d).

Moreover, viscosities of both pure VG 220 oil and 0.1 wt.% PMMA/CQDs in VG 220 oil were recorded at both 100°C and 40°C and values were reported in Figure 13. As can be seen, no significant modifications of viscosity could be detected between the two samples, which confirmed that the presence of small percentages of the nanocomposite in the oil did not significantly modify its rheological property.

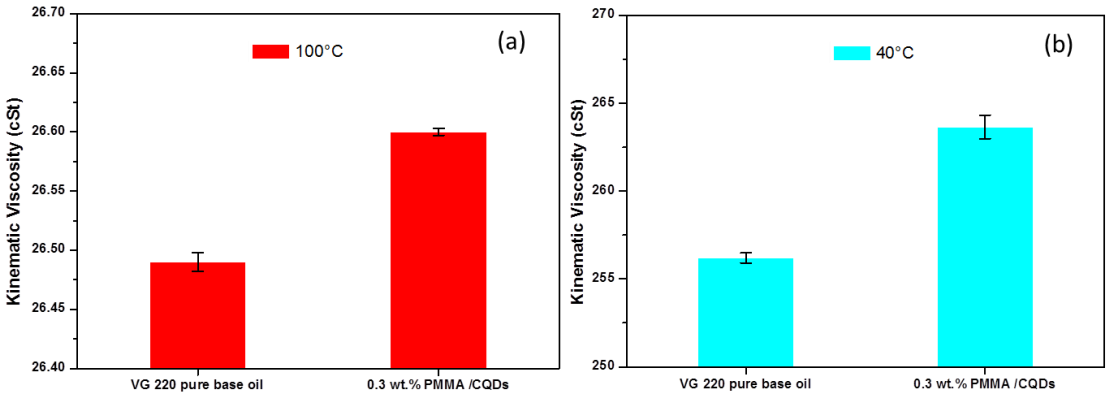

Figure 13. Kinematic viscosities at a) 100°C and b) 40°C for both 0.3 wt. % PMMA/CQDs +VG 220 and pure VG 220.

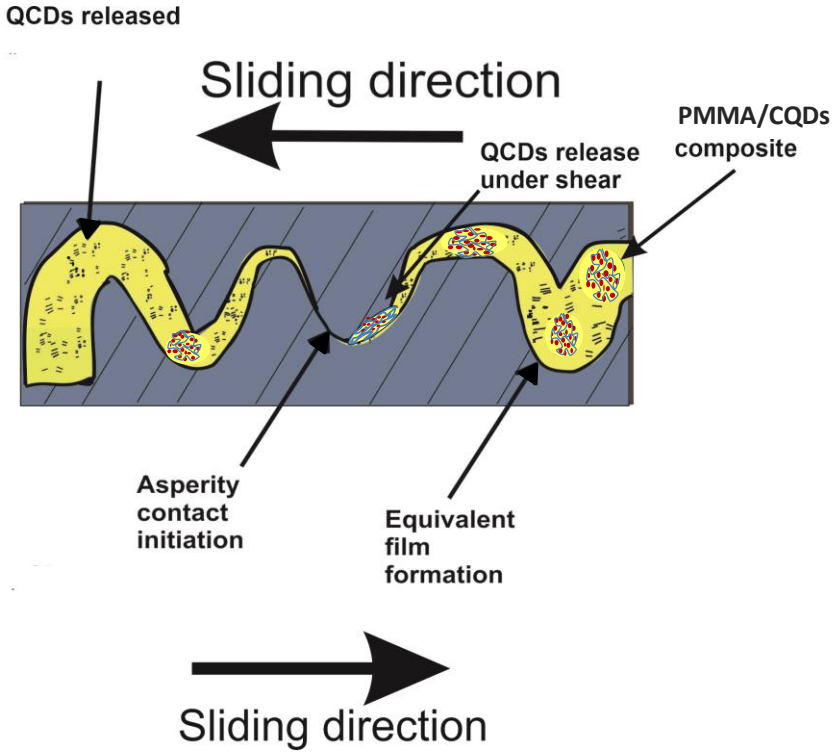

Figure 14. Proposed tribological mechanism of the PMMA/CQDs nanocomposite.

Eventually, considering the aforementioned results, the PMMA/CQDs composite was able to enhance the tribological performance of the pure commercial oil as a consequence of: a) the release of the entrapped CQDs from the polymer structure under lubrication conditions; and, b) the subsequent efficient lubricating mechanism of the quantum dots, free to interact with their hydrophilic groups with the metal surface to lubricate. A comprehensive scheme of the lubrication mechanism is shown in Figure 14. The metal surface, due to emission of low-energy electrons, is, during friction, positively charged and suitable to adsorb CQDs functionalities. As suggested by the behavior showed under time increase, at the initial stage, CQDs act as bearing balls decreasing

friction, while continuous deposition results in the formation of a protective film reducing the direct contact between the friction pairs. Further analyses have been planned and are required to completely clarify the lubrication mechanism, by also deeply analyzing the wear track morphology.

4. Conclusion

In summary, PMMA/CQDs composite, consisting of carbon quantum dots, 1-2 nm average diameter, entrapped in a PMMA matrix, was prepared through a one-step, mild temperature, oleic acid- and citric acid-based *green* synthesis. PMMA not only ensures CQDs long-time stability in non-polar commercial oils but, at the same time, allows the release of CQDs under lubricated equipment's operating conditions. Tribological tests carried out in a VG 220 commercial mineral oil confirmed the high anti-wear and anti-friction performance of the synthesized sample. CQDs, acting as bearing balls on the positively charged surface, decrease friction, whereas continuous deposition results in the formation of a protective film, which significantly reduces the direct contact between the friction pairs. In this context, it is of high importance the CQDs homogenous suspension, for a continuous supply after deposition and shearing.

Viscosity measurements at 40°C and 100°C confirmed that the presence of small percentages of the nanocomposite in the oil did not significantly change its rheological property. This is particularly interesting because it does not interfere with the physical properties of the base oil, as well as with the delicate balance of the final industrial formulations. Obviously, by increasing the PMMA amount, an improvement of the VI of the fully-formulated oil is expected to occur, which can affect only positively the CQDs dispersion.

Acknowledgements

This research was supported by National Operative Programme for Companies and Competitiveness 2014−2020 - Horizon 2020, funded by the European Union (Rilub SPA, project leader. Project n. F/050190/01-02/x32 – Introduzione di nanotecnologie e materiali avanzati nel settore industrial delle trasmissioni meccaniche di Potenza e, in particolare, dei lubrificanti per gli ingranaggi – INNOLUBE).

References

[1] Studt P. Boundary lubrication: adsorption of oil additives on steel and ceramic surfaces and its influence on friction and wear. Tribol Int 1989;22:111-119. https://doi.org/10.1016/0301-679X(89)90171-0.

[2] Bouchet MDB, Martin JM, Le Mogne T, Bilas P, Vacher B, Yamada Y. Mechanisms of MoS_2 formation by MoDTC in presence of ZnDTP: effect of oxidative degradation. Wear 2005;258:1643-1650. https://doi.org/10.1016/j.ear.2004.11.019.

[3] Forbes ES. Antiwear and extreme pressure additives for lubricants. Tribology 1970;3:145-152. https://doi.org/10.1016/0041-2678(70)90111-9.

[4] Bakunin VN, Suslov AY, Kuzmina GN, Parenago OP, Topchiev AV. Synthesis and application of inorganic nanoparticles as lubricant components–a review. J Nanoparticle Res 2004;6:273-284. https://doi.org/10.1023/B:NANO.0000034720.79452.e3.

[5] Zhang W, Demydov D, Jahan MP, Mistry, K, Erdemir, A, Malshe, AP. Fundamental understanding of the tribological and thermal behavior of Ag–MoS_2 nanoparticle-based multi-component lubricating system. Wear 2012;288:9-16. https://doi.org/10.1016/j.wear.2012.03.003

[6] Jiao D, Zheng S, Wang Y, Guan R, Cao B. The tribology properties of alumina/silica composite nanoparticles as lubricant additives. Appl Surf Sci 2011;257:5720-5725. https://doi.org/10.1016/j.apsusc.2011.01.084.

[7] Sarno M, Senatore A, Cirillo C, Petrone V, Ciambelli P. Oil lubricant tribological behaviour improvement through dispersion of few layer graphene oxide. J Nanosci Nanotechnol 2014; 4:4960-4968. https://doi.org/10.1166/jnn.2014.8673.

[8] Spikes H. Friction modifier additives. Tribol Lett 2015;60:5. DOI: 10.1007/s11249-015-0589-z.

[9] Grierson DS, Carpick RW. Nanotribology of carbon-based materials. Nano Today 2007;2:12-21. https://doi.org/10.1016/S1748-0132(07)70139-1.

[10] Min C, Liu D, Shen C, Zhang Q, Song H, Li S, Shen X, Zhu M, Zhang K. Unique synergistic effects of graphene oxide and carbon nanotube hybrids on the tribological properties of polyimide nanocomposites. Tribol Int 2018;117:217-224. https://doi.org/10.1016/j.triboint.2017.09.006.

[11] Cumings J, Zettl A. Low-friction nanoscale linear bearing realized from multiwall carbon nanotubes. Science 2000;289:602-604. DOI: 10.1126/science.289.5479.602.

[12] Sharma AK, Tiwari AK, Dixit AR, Singh RK, Singh M. Novel uses of alumina/graphene hybrid nanoparticle additives for improved tribological properties of lubricant in turning operation. Tribol Int 2018;119:99-111. https://doi.org/10.1016/j.triboint.2017.10.036.

[13] Singh RK, Sharma AK, Dixit AR, Tiwari AK, Pramanik A, Mandal A. Performance evaluation of alumina-graphene hybrid nano-cutting fluid in hard turning. J Clean Prod 2017;162:830-845. https://doi.org/10.1016/j.jclepro.2017.06.104.

[14] Elomaa O, Singh VK, Iyer A, Hakala TJ, Koskinen J. Graphene oxide in water lubrication on diamond-like carbon vs. stainless steel high-load contacts. Diam Relat Mater 2015;52:43-48. https://doi.org/10.1016/j.diamond.2014.12.003.

[15] Wu H, Zhao J, Xia W, Cheng X, He A, Yun JH, Wang L, Huang H, Jiao S, Huang L, Zhang S. A study of the tribological behaviour of TiO_2 nano-additive water-based lubricants. Tribol Int 2017;109:398-408. https://doi.org/10.1016/j.triboint.2017.01.013.

[16] Muthuvel S, Naresh Babu M, Muthukrishnan N. Copper nanofluids under minimum quantity lubrication during drilling of AISI 4140 steel. Aust J Mech Eng 2018;1-14. https://doi.org/10.1080/14484846.2018.1486694.

[17] Shahnazar S, Bagheri S, Hamid SBA. Enhancing lubricant properties by nanoparticle additives. Int J Hydrog Energy 2016;41:3153-3170. https://doi.org/10.1016/j.ijhydene.2015.12.040.

[18] Chen CS, Chen XH, Xu LS, Yang Z, Li WH. Modification of multi-walled carbon nanotubes with fatty acid and their tribological properties as lubricant additive. Carbon 2005;43:1660-1666. https://doi.org/10.1016/j.carbon.2005.01.044.

[19] Zhang W, Zhou M, Zhu H, Tian Y, Wang K, Wei J, Ji F, Li X, Li Z, Zhang P, Wu D. Tribological properties of oleic acid-modified graphene as lubricant oil additives. J Phys D 2011;44:205303. https://doi.org/10.1088/0022-3727/44/20/205303.

[20] Lin J, Wang L, Chen G. Modification of graphene platelets and their tribological properties as a lubricant additive. Tribol Lett 2011;41:209-215. https://doi.org/10.1007/s11249-010-9702-5.

[21] Ota J, Hait SK, Sastry MIS, Ramakumar SSV. Graphene dispersion in hydrocarbon medium and its application in lubricant technology. RSC Adv 2015;5:53326-53332. https://doi.org/10.1039/C5RA06596H.

[22] Xu X, Ray R, Gu Y, Ploehn HJ, Gearheart L, Raker K, Scrivens WA. Electrophoretic analysis and purification of fluorescent single-walled carbon nanotube fragments. J Am Chem Soc 2004;126:12736-12737. https://doi.org/10.1021/ja040082h.

[23] Jia X, Li J, Wang E. One-pot green synthesis of optically pH-sensitive carbon dots with upconversion luminescence. Nanoscale 2012;4:5572-5575. https://doi.org/10.1039/C2NR31319G.

[24] Jiang, F, Chen D, Li R, Wang Y, Zhang G, Li S, Zheng J, Huang N, Gu Y, Wang C, Shu C. Eco-friendly synthesis of size-controllable amine-functionalized graphene quantum dots with antimycoplasma properties. Nanoscale 2013;5:1137-1142. https://doi.org/10.1039/C2NR33191H.

[25] Dong Y, Wang R, Li H, Shao J, Chi Y, Lin X, Chen G. Polyamine-functionalized carbon quantum dots for chemical sensing. Carbon 2012;50:2810-2815. https://doi.org/10.1016/j.carbon.2012.02.046.

[26] De B, Karak N. A green and facile approach for the synthesis of water soluble fluorescent carbon dots from banana juice. RSC Adv 2013;3:8286-8290. https://doi.org/10.1039/C3RA00088E.

[27] Gao S, Chen Y, Fan H, Wei X, Hu C, Wang L, Qu L. A green one-arrow-two-hawks strategy for nitrogen-doped carbon dots as fluorescent ink and oxygen reduction electrocatalysts. J Mater Chem A 2014;2:6320-6325. https://doi.org/10.1039/C3TA15443B.

[28] Saxena M, Sarkar S. Fluorescence imaging of human erythrocytes by carbon nanoparticles isolated from food stuff and their fluorescence enhancement by blood plasma. Mater Res Express 2013;3:201-209. https://doi.org/10.1166/mex.2013.1126.

[29] Krysmann MJ, Kelarakis A, Giannelis EP. Photoluminescent carbogenic nanoparticles directly derived from crude biomass. Green Chem 2012;14:3141-3145. https://doi.org/10.1039/C2GC35907C.

[30] Dong Y, Wang R, Li H, Shao J, Chi Y, Lin X, Chen G. Polyamine-functionalized carbon quantum dots for chemical sensing. Carbon 2012;50:2810-2815. https://doi.org/10.1016/j.carbon.2012.02.046.

[31] Wang F, Pang S, Wang L, Li Q, Kreiter M, Liu CY. One-step synthesis of highly luminescent carbon dots in noncoordinating solvents. J Mater Chem 2010;22:4528-4530. https://doi.org/10.1021/cm101350u.

[32] Bourlinos AB, Stassinopoulos A, Anglos D, Zboril R, Karakassides M, Giannelis EP. Surface functionalized carbogenic quantum dots. Small 2008;4:455-458. https://doi.org/10.1002/smll.200700578.

[33] Ye M, Cai T, Zhao L, Liu D, Liu S. Covalently attached strategy to modulate surface of carbon quantum dots: Towards effectively multifunctional lubricant additives in polar and apolar base fluids. Tribol Int 2019;136:349-359. https://doi.org/10.1016/j.triboint.2019.03.045.

[34] Tu Z, Hu E, Wang B, David KD, Seeger P, Moneke M, Stengler R, Hu K, Hu X. Tribological behaviors of Ni-modified citric acid carbon quantum dot particles as a green additive in polyethylene glycol. Friction 2020;8:182-197. https://doi.org/10.1007/s40544-019-0272-8.

[35] Johnson JR, Schober BJ. Lubrizol Corp, U.S. Patent Application No. 14/416,785. 2015.

[36] Selby TW. The non-Newtonian characteristics of lubricating oils. ASLE Trans 1958;1:68-81. https://doi.org/10.1080/05698195808972315.

[37] Rizvi SQA. Additives for automotive fuels and lubricants. Tribol Lubr Technol 1999;55:33.

[38] Aziz SB, Abdullah OG, Brza MA, Azawy AK, Tahir DA. Effect of carbon nano-dots (CNDs) on structural and optical properties of PMMA polymer composite. Results Phys 2019;15:102776.

[39] Maxim AA, Sadyk SN, Aidarkhanov D, Surya C, Ng A, Hwang YH, Atabaev TS, Jumabekov AN. PMMA Thin Film with Embedded Carbon Quantum Dots for Post-Fabrication Improvement of Light Harvesting in Perovskite Solar Cells. Nanomaterials-Basel 2020;10:291.

[40] Bouknaitir I, Panniello A, Teixeira SS, Kreit L, Corricelli M, Striccoli M, Costa LC, Achour ME. Optical and dielectric properties of PMMA (poly (methyl methacrylate))/carbon dots composites. Polym Compos 2019;40:E1312-E1319.

[41] Sarno M, Senatore A, Spina D, Mustafa WAAA. Tribochemical Boost for Cu Based Lubricant Nano-Additive. Key Eng Mater 2019;813:292–297. https://doi.org/10.4028/www.scientific.net/KEM.813.292.

[42] Sarno M, Spina D, Senatore A. One-step nanohybrid synthesis in waste cooking oil, for direct lower environmental impact and stable lubricant formulation. Tribol Int 2019;135:355-367. https://doi.org/10.1016/j.triboint.2019.03.025.

[43] Gugula K, Bredol M. Transparent $CuInS_2$/PMMA Nanocomposites Luminescent in the Visible and NIR Region. Z Naturforsch 2014;69b:217-223. https://doi.org/10.5560/znb.2014-3264.

[44] Bhunia SK, Saha A, Maity AR, Ray SC, Jana NR. Carbon nanoparticle-based fluorescent bioimaging probes. Sci Rep 2013;3:1473. https://doi.org/10.1038/srep01473.

[45] El-Zaher NA, Osiris WG. Thermal and structural properties of poly (vinyl alcohol) doped with hydroxypropyl cellulose. J Appl Polym Sci 2005;96:1914-1923. https://doi.org/10.1002/app.21628.

[46] Yaragalla S, Anilkumar G, Kalarikkal N, Thomas S. Structural and optical properties of functionalized multi-walled carbon nanotubes. Mater Sci Semicond Process 2016;41:491-496. https://doi.org/10.1016/j.mssp.2015.10.022.

[47] Aziz SB, Hassan AQ, Mohammed SJ, Karim WO, Kadir MFZ, Tajuddin HA, Chan NNMY. Structural and optical characteristics of PVA: C-Dot composites: Tuning the absorption of ultra violet (UV) region. J Nanomater. 2019;9:216. https://doi.org/10.3390/nano9020216.

[48] Aziz SB, Hassan AQ, Mohammed SJ, Karim WO, Kadir MFZ, Tajuddin HA, Chan NNMY. Structural and optical characteristics of PVA: C-Dot composites: Tuning the absorption of ultra violet (UV) region. Nanomater 2019;9:216. https://doi.org/10.3390/nano9020216.

[49] Aziz SB, Abdullah OG, Brza MA, Azawy AK, Tahir DA. Effect of carbon nano-dots (CNDs) on structural and optical properties of PMMA polymer composite. Results Phys 2019;15:102776. https://doi.org/10.1016/j.rinp.2019.102776.

[50] Ahmed RM. Optical study on poly (methyl methacrylate)/poly (vinyl acetate) blends. Int J Photoenergy 2009;2009:150389. https://doi.org/10.1155/2009/150389.

[51] Ye M, Cai T, Shang W, Zhao L, Zhang Y, Liu D, Liu S. Friction-induced transfer of carbon quantum dots on the interface: Microscopic and spectroscopic studies on the role of inorganic–organic hybrid nanoparticles as multifunctional additive for enhanced lubrication. Tribol Int 2018;127:557-567. https://doi.org/10.1016/j.triboint.2018.06.033.

[52] Luo T, Wei X, Huang X, Huang L, Yang F. Tribological properties of Al_2O_3 nanoparticles as lubricating oil additives. Ceram Int 2014;40:7143-7149. https://doi.org/10.1016/j.ceramint.2013.12.050.

[53] Wan Q, Jin Y, Sun P, Ding Y. Tribological behaviour of a lubricant oil containing boron nitride nanoparticles. Procedia Eng 2015;102:1038-1045. https://doi.org/10.1016/j.proeng.2015.01.226.

[54] Yu R, Liu J, Zhou Y. Experimental study on tribological property of MoS_2 nanoparticle in castor oil. J Tribol 2019;141:102001. https://doi.org/10.1115/1.4044294.

[55] Kaviyarasu T, Vasanthan B. Improvement of tribological and thermal properties of engine lubricant by using nano-materials. J Chem Pharm Sci 2015;7:208-211. https://www.jchps.com/specialissues/Special%20issue%207/53%20MITNC-59%20Kaviyarasu%20T%20208-211.pdf

[56] McFarlane JS, Tabor D. Junction Growth in Metallic Crystals. P Roy Soc A-Math Phy 1950;202:244-253. https://doi.org/10.1098/rspa.1959.0114.

[57] Mungse HP, Khatri OP. Chemically functionalized reduced graphene oxide as a novel material for reduction of friction and wear. J Phys Chem C 2014;118:14394-14402. https://doi.org/10.1021/jp5033614.